On Selecting the Size of a Spacecraft's Buffer

Shervin Shambayati*

As NASA moves to Ka-band (32-GHz) and optical deep space missions, adverse weather events threaten the completeness of the received data. A retransmission scheme can assure data completeness, but requires additional link capacity and storage. This article examines the fundamental trade-off between spacecraft buffer size and link capacity, and its effect on the data loss rate. Using a Markovian model to characterize the amount of data stored in the buffer, we found that (a) a large buffer size mitigates many problems associated with changes in mission data loss requirements and inaccurate link modeling, (b) more frequent but shorter passes reduce data losses but adds to the cost of spacecraft tracking and may violate the assumptions of the model, and (c) at short distances data loss process is dominated by the size of the buffer and equipment availability while at longer distances the process is dominated by the average link capacity.

I. Introduction

Recently, NASA has been interested in using Ka-band (32 GHz) and optical frequencies for receiving data from its deep space probes. This interest is due to the fact that these frequencies can, on the average, return more data from the spacecraft than the current X-band (8.41 GHz) frequency for the same amount of tarnsmitted power from the spacecraft [1, 2, 3]. However, this increase in the average data volume is achieved only if the reliability of the link is significantly reduced. This lower reliability causes discontinuities in the data. To solve this problem it is assumed that if the data are not correctly received on the ground they would be saved onboard the spacecraft for retransmission at a later time. Inherent in this assumption are two aspects: 1. Excess channel capacity exists on the link to support these retransmissions. 2. There is enough storage onboard the spacecraft to accommodate the data to be retransmitted. Both these assumptions mean that additional resources are necessary onboard the spacecraft. In order to minimize the cost we need to quantify the minimum resources that are necessary in order to achieve a required data loss rate. In this paper we introduce a general Markovian model for the amount of data in the spacecraft buffer and derive the equations for its

*Communications Architectures and Research Section. The research described in this publication was carried out by the Jet Propulsion Laboratory, California Institute of Technology, under a contract with the National Aeronautics and Space Administration

Markov transition matrix in Section II. Using this matrix, equations for the data loss rate and capacity utilization rate are derived. Next, in Section III, this approach is used to derive equations for a specific fixed-rate data collection/modified binomial capacity (FRDC/MBC) model. The characteristics of the FRDC/MBC along with their implications for system design are discussed in Section IV. In Section V FDCR/MBC model is applied to two proposed system designs for the Space Interferometry Mission (SIM) to analyze their performance over the life of the mission. Next the caveats are presented in Section VI. In the last section conclusions are summarized.

II. The General Markov Model

Consider the amount of data in a spacecraft buffer at the end of the lth pass, B_l. Let A_{l+1} be the amount of data that the spacecraft accumulates between the lth and $l+1$st pass and C_{l+1} be the amount data that could be communicated successfully during the $l+1$st pass. If the spacecraft buffer size is m then B_l satisfies the following recurrence equation:

$$B_{l+1} = \max\left[\min\left(B_l + A_{l+1}, m\right) - C_{l+1}, 0\right] \tag{1}$$

If A_ls and C_ls are each non-negative integers (that is, data is packetized into data units) and independently and identically distributed then B_l constitutes a Markov Jump Process [4]. The transition matrix for this jump process, $\mathbf{P} = \{p_{ij}\}$ is given by:

$$p_{ij} = \begin{cases} \sum_{n=0}^{m-i} \Pr\{A = n\} \Pr\{C \geq i + n\} & j = 0 \\ \quad + \Pr\{A > m - i\} \Pr\{C \geq m\} & \\ \sum_{n=\max(j-i,0)}^{m-i} \Pr\{A = n\} \Pr\{C = n + i - j\} & 0 < j \leq m \\ \quad + \Pr\{A > m - i\} \Pr\{C = m - j\} & \\ 0 & \text{otherwise} \end{cases} \tag{2}$$

Using equation 2 the steady-state distribution of B, $\mathbf{\Pi} = \{\pi(i) = \Pr\{B_\infty = i\}\}$, could be easily calculated. Given $\mathbf{\Pi}$, the data loss rate–also known as the blocking probability–is given by:

$$P_B = \frac{\sum_{i=0}^{m} \pi(i) \sum_{j=m-i+1}^{\infty} (i + j - m) \Pr\{A = j\}}{\sum_{l=1}^{\infty} l \Pr\{A = l\}} \tag{3}$$

Aside from the blocking probability an important measure of performance is the link utilization rate. This indicates how efficient the overall system design is in terms of using its allocated resources. Let $\mathbf{P} = \{P(i)\}$ be the steady-state probability distribution of the

number of data units in the spacecraft buffer at the beginning of a pass. $P(i)$ is given by:

$$P(i) = \begin{cases} \sum_{j=0}^{i} \pi(j) \Pr\{A = i - j\} & i < m \\ \sum_{j=0}^{m} \pi(j) \Pr\{A \geq m - j\} & i = m \\ 0 & \text{otherwise} \end{cases} \quad (4)$$

Then the utilization rate per pass over which a successful transmission may occur is given by:

$$U_t = \sum_{j=1}^{\infty} \sum_{i=0}^{m} P(i) \frac{\Pr\{C = j\}}{1 - \Pr\{C = 0\}} \frac{\min(j, i)}{j} \quad (5)$$

In the following sections these equations are used for a specific model to design and analyze end-to-end spacecraft telecommunication systems in terms of their data loss rate and their capacity utilization rate.

III. Fixed-Rate Data Collection/Modified Binomial Capacity (FRDC/MBC) Model

Consider the case where the distribution of the number data units that arrive between two passes is given by:

$$\Pr\{A = j\} = \begin{cases} 1 & j = j_0 \\ 0 & \text{otherwise} \end{cases} \quad (6)$$

and a link capacity distribution given by:

$$\Pr\{C = l\} = \begin{cases} (1 - p_1) + (1 - p)^w - (1 - p_1)(1 - p)^w & l = 0 \\ \binom{w}{q} p_1 (1 - p)^{w-q} p^q & l = qr, q = 1, 2, \ldots w \\ 0 & \text{otherwise} \end{cases} \quad (7)$$

then equation 2 takes the form

$$p_{ij} = \begin{cases} \sum_{q=\left\lceil \frac{\min(i+j_0, m)}{r} \right\rceil}^{w} \binom{w}{q} (1 - p)^{w-q} p^q p_1 & j = 0 \\ (1 - p_1) + (1 - p)^w - (1 - p_1)(1 - p)^w & j = \min(i + j_0, m) \\ \binom{w}{q} (1 - p)^{w-q} p^q p_1 & j = \min(i + j_0, m) - qr, \\ & q =, 1, 2, \ldots, w \\ 0 & \text{otherwise} \end{cases} \quad (8)$$

The model represented by the above equations is called the Fixed-Rate Data Collection/Modified Binomial Capacity (FRDC/MBC) model. This model assumes that the spacecraft collects the same amount of data–called a "contact"– between two passes. It also assume that the pass capacity is determined by two independent processes: a Bernoulli process with parameter p_1 and binomial process with parameters p and w. While this model is rather simple many deep-space missions fit this model rather well. These missions are those where the spacecraft collects the same type of data over and over again and it has regularly scheduled passes over the Deep Space Network (DSN). Among these missions are observatory-like spacecraft such as the Space Interferometry Mission (SIM), Kepler and James Webb Space Telescope (JWST) and orbiters such as Mars Reconnaissance Orbiter (MRO).

These missions typically have one instrument (usually a camera or something similar) that generates almost all of the data that the spacecraft needs to transmit. Furthermore, the nature of the observations made by this instrument does not change fundamentally over the life of the mission. This type of mission collects data at a constant rate over long periods of time and only when fundamental changes in the scientific goals of the mission are made this data collection rate changes. Since the amount of data collected by these missions remain relatively constant, the DSN can allocate regularly scheduled assets to them to support their data downlinks.

However, allocation of DSN assets does not necessarily mean that a fixed capacity is available on a regular basis. There are two main factors that prevent availability of a fixed capacity over the link. The first is equipment failure. DSN assets are guaranteed to be 95% reliable. Therefore, at most 5% of the passes are lost due to ground equipment failure. In addition, adverse weather increases the system noise temperature, thus degrading the link performance. When DSN equipments fail, the failure usually lasts a few days. Therefore, if a DSN asset breaks down for a pass, that pass is assumed lost. Assuming independence of failures (that is, if an asset breaks down it does not affect availability of the asset for the next scheduled pass), the breaking down process of a DSN asset can be modeled as a Bernoulli process.

Adverse weather effects manifest themselves in terms of degradation of the link performance. An initial analysis of the link outages has been performed [7]. This analysis indicates that adverse weather events could last for several hours. If there is no way to adjust the data rate to combat these effects, large portions of a pass could be lost. Assuming that independent adverse weather events have roughly the same duration, then it could be assumed that a given pass consists of multiple independent segments of roughly equal length corresponding to the duration of an adverse weather event that, for a given link design, have equal availability (this is a very rough approximation because as the elevation increases during the pass, the system noise temperature decreases and thus the link can either support higher data rates or achieve greater availability). Therefore, when the DSN assets are available, the capacity of the link could be modeled as a binomial process.

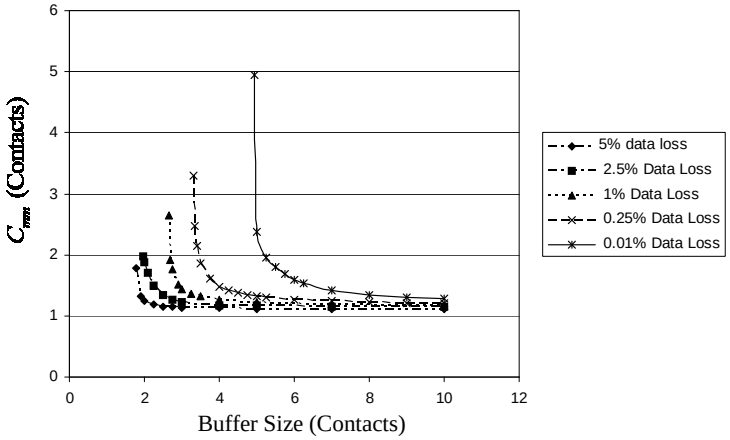

Figure 1. C_{mm} vs. buffer size for different data loss rate requirements. One segment per pass. 85% total pass availabilty

Using this model, one can design an end-to-end communications system for a given data loss rate. Conversely, this model could be used to evaluate the performance of an existing system. In the next two sections each of these methods of analysis is discussed.

IV. Characteristics of FRDC/MBC Model and System Design Implications

Typically, deep space missions are asked to provide a certain data loss rate for the life of the mission. Given an equipment availability, p_1 and a given segment availability p, there are many combinations of spacecraft buffer size and minimum segment capacity that satisfy the data loss rate requirement of P_b. Plots of minimum segment capacity vs. spacecraft buffer size could be generated easily using the equations from the previous sections. However, most telecom system designers are concerned with the total pass capacity when the pass is completely available. Therefore, we define the minimum maximum Capacity (*i.e.,* the minimum required pass capacity if all segements are available), C_{mm}, as

$$C_{mm} = wC_{sm} \tag{9}$$

where w is the number of independent segments per pass and C_{sm} is the minimum required segment capacity when the segment is available. Plotting C_{mm} vs. the buffer size for different values of w, p, p_1 and P_b different system designs and assumptions could be compared with each other.

One of the fundamental assumptions in the FRDC/MBC model is that spacecraft collects the same amount of new data between passes. As mentioned before, this amount, j_0, is referred to as a "contact." Given this assumption, C_{mm} and the buffer size, m, could be normalized to "contacts" and curves of C_{mm} vs. m for fixed values of P_b could be plotted. Examples of these plots are shown in figures 1 through 3.

Before discussing each figure in detail it should be noted that each curve in these figures has a vertical and a horizontal asymptote. The horizontal asymptote is the C_{mm} required to successfully receive $1 - P_b$ of the data collected by the spacecraft if the spacecraft has an infinite size buffer. The value of this asymptote, a_h, is easily calculated according to

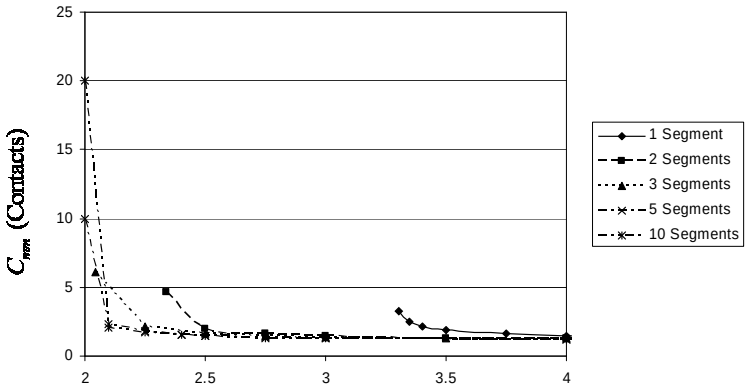

(a) Smaller Buffer Sizes

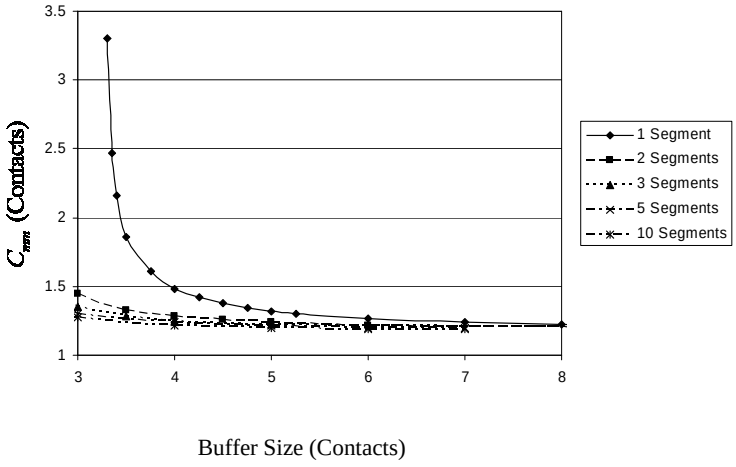

(b) Larger Buffer Sizes

Figure 2. C_{mm} **vs. buffer size for different numbers of segments per pass,** p**=0.895,** p_1**=0.95, 0.25% data loss rate**

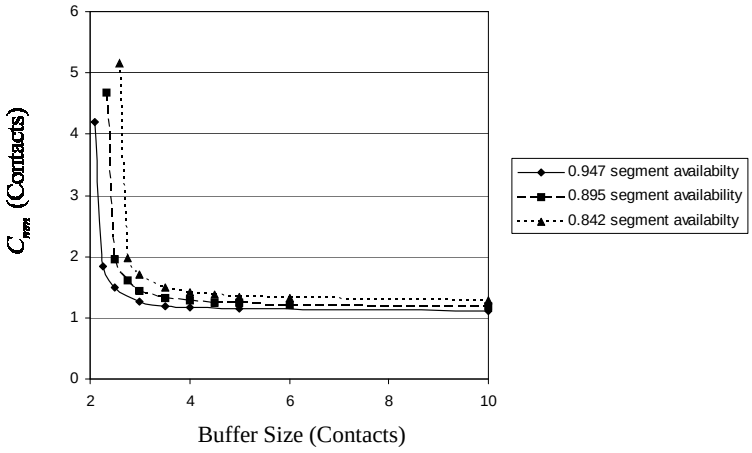

(a) 0.25% data loss rate

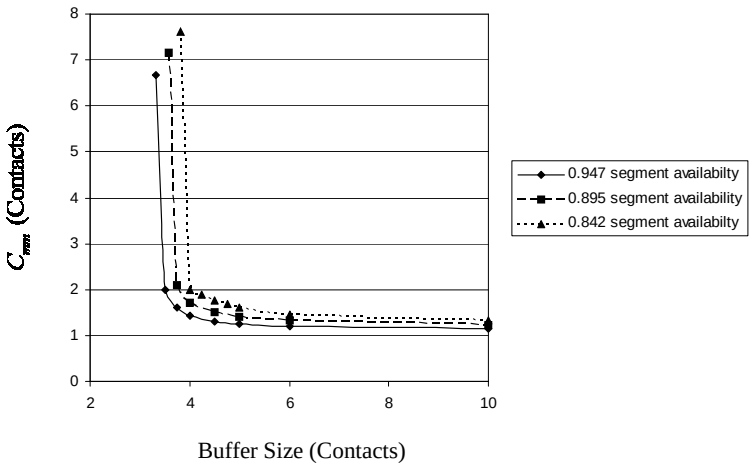

(b) 0.01% data loss rate

Figure 3. C_{mm} vs. buffer size for different segment availability values, 2 segments per pass, 95% equipment availability

the following:

$$a_h = \frac{1 - P_b}{p_1 \cdot p} \tag{10}$$

While the vertical asymptote is not as easily calculated as the horizontal asymptote, it is just as easily explained. Each curve merges with its vertical asymptote when the $C_{sm} = m$. The curve merges with this asymptote because the data loss performance of the system is the same for $C_{sm} \geq m$ as each available segment is capable of emptying the maximum amount of data that the buffer may contain. Therefore, for a given data loss rate, P_b, the minimum required buffer size, $m_{\min}$, must satisfy the following equality:

$$P_b = \left(\left\lceil \frac{m_{\min}}{j_0} \right\rceil - \frac{m_{\min}}{j_0} \right) p_0^{\lfloor m_{\min}/j_0 \rfloor} (1 - p_0) + p_0^{\lceil m_{\min}/j_0 \rceil} \tag{11}$$

where p_0, the probability that no data could be transmitted over a pass, is given by:

$$p_0 = (1 - p_1) + p_1(1 - p)^w \tag{12}$$

and j_0 is the amount of data in a contact.

The figures themselves are meant to explore the effects of the following on the tradeoff between the buffer size and the required capacity:

- Changes in the data loss requirement.
- Changes in the number of independent segments in a pass.
- Changes in the availability of the segments.

Figure 1 shows the effects of reducing the data loss requirement from 5% to 0.01% for a pass that consists of one segment with an overall availability of 0.85. Note that in this case since the pass consists of one segment, the equipment availability, p_1, and the weather availability, p, could be combined into a single number. As seen from Figure 1, as the data loss requirement becomes more stringent the required minimum buffer size (the vertical asymptote) increases. In addition, if buffer size is relatively small (but greater than the minimum required buffer size), a more stringent data loss requirement could significantly increase the required C_{mm} capacity.

To investigate how the assumptions about the number of independent segments per pass affect the buffer size/link capacity tradeoff, C_{mm} curves for different numbers of segments for a data loss rate of 0.25% with a segment availability of $p = 0.895$ and an equipment availability of $p_1 = 0.95$ were calculated. Note that for the same C_{mm} value, the average capacity per pass is the same regardless of the number of segments per pass. This allows a fair comparison of the assumptions for the number of independent segments per pass.

The results of these calculations are shown in Figures 2a and 2b. As seen from Figure 2a, there is a substantial reduction in the minimum required buffer size when the number of independent segments per pass is increased from 1 to 2. However, there is no such dramatic change in the minimum required buffer size when going from 2 segments to 10 segments

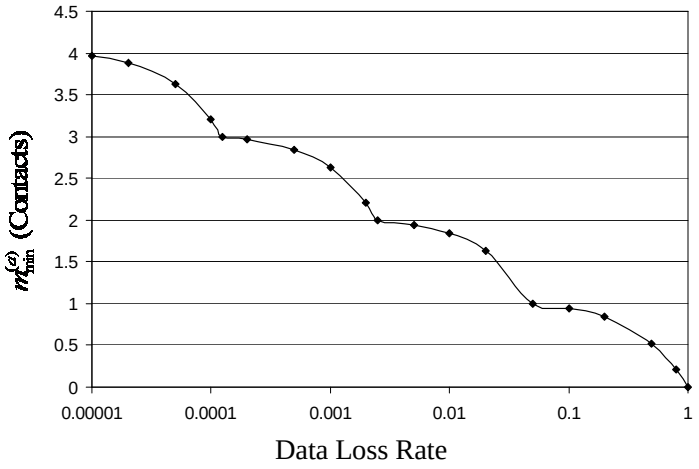

Figure 4. $m_{\min}^{(a)}$ **vs. data loss rate for 95% equipment availability (**p_1**).**

per pass. There is no change because the minimum buffer size achieves the required the data loss rate if and only if a segment has the capacity to empty the entire buffer. As the number segments, w, increases, p_0 in equation 12 approahes $1 - p_1$. Therefore, as the number of segments increases, the minimum required buffer size is determined by the equipment availability. Since it is assumed that the equipment availability is independent of the number of segments in a pass, as the number of segments increases the minimum required buffer size converges to a value, $m_{\min}^{(a)}$ which satisfies the following equality:

$$P_b = \left(\left\lceil \frac{m_{\min}^{(a)}}{j_0} \right\rceil - \frac{m_{\min}^{(a)}}{j_0} \right) p_1 (1-p_1)^{\left\lfloor m_{\min}^{(a)}/j_0 \right\rfloor} + (1-p_1)^{\left\lceil m_{\min}^{(a)}/j_0 \right\rceil} \tag{13}$$

Figure 4 shows $m_{\min}^{(a)}$ vs. data loss rate for p_1=0.95. Note that the stepwise characteristic of this curve arise from the ceiling and floor function in equation 13.

Furthermore, Figure 2a indicates that when the buffer size is relatively small, the assumption about the number of independent segments per pass could substantially change the value of C_{mm}. However, as Figure 2b shows, for larger buffer sizes (greater than 5.5 contacts in this case) the assumptions about the number of independent segments has very little effect on the value of C_{mm}.

Figures 3a and 3b show the effects of changes in the segment availability on the C_{mm} curves. Figure 3a shows the C_{mm} curves assuming 2 segments per pass and 95% equipment availability for the segment availabilities of 0.947, 0.895 and 0.842 for a data loss rate 0f 0.25 %. Figure 3b shows the same for a data loss rate of 0.01%. The segment availabilities were chosen so that the average capacities per pass are $0.9C_{mm}$, $0.85C_{mm}$ and $0.8C_{mm}$, repsectively. As seen from these figures, as the buffer size increases, there is less of a difference between the C_{mm} values for the different availabilities. However, as the data loss rate requirement becomes more stringent the difference between the C_{mm} curves for different availabilities becomes more pronounced.

The characteristics of the capacity utilization rate for this model are illustrated in Figures 5 through 7. Figure 5 indicates that the smaller the data loss rate requirement, the lower is the capacity utilization rate. This is due to the fact that the lower data loss

requirements require higher capacity for the same buffer size. However, this excess capacity is very rarely used. Therefore, the utilization rate drops as the data loss requirement becomes more stringent. Figure 6 shows the effects of changing the assumption about the number of independent segments in each pass. As this figure indicates, for the same buffer size the larger the number of segments per pass the higher is the utilization rate. This is due to the fact that, as Figure 2a indicates, the larger number of segments requires less capacity for the same data loss rate and the same buffer size. Since the amount of data transmitted is the same on the average, the capacity utilization rate is higher for the larger number of segments per pass. Similarly, as the per segment availability increases so does the capacity utilization rate for the same buffer size(Figure 7). This indicates that even though the average amount of data in the buffer decreases with the higher segment availability, the decrease in C_{mm} is even greater for the same buffer size thus increasing the capacity utilization rate. It should be noted that in all cases as the buffer size increases the capacity utilization rate increases as well and the difference between the utilization curves in Figures 5 through 7 becomes less.

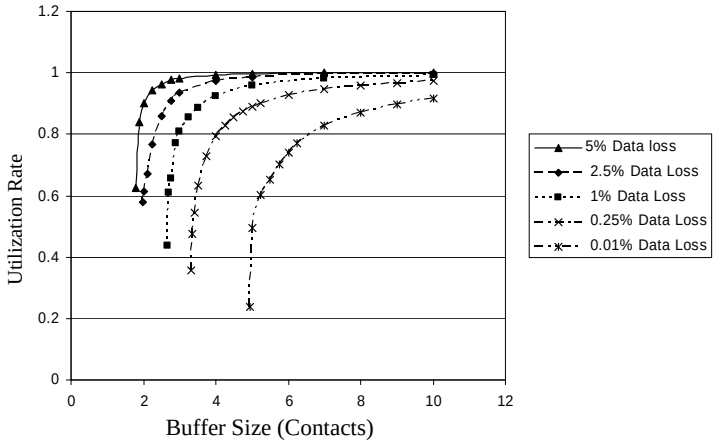

Figure 5. Capacity utilization rate vs. buffer size for different data loss rate requirements. One segment per pass. 85% total pass availability

If there is a common theme that runs through the analysis of Figures 1 through 7 is that a larger buffer size allows small increases in the C_{mm} to compensate for the inaccurate modeling of the channel availability or changes in the data loss requirement. It should also be noted that for a given spacecraft telecom system with a fixed equivalent isotropic radiated power (EIRP) at a given distance from Earth, as the data rate increases, the link availibility decreases. Therefore,the job of spacecraft designer is not just to pick a point on a C_{mm} curve but rather to evaluate combinations of EIRP and buffer size and see which combinations meet the data loss rate goals of the mission and how. In the next section an example of such an analysis is given.

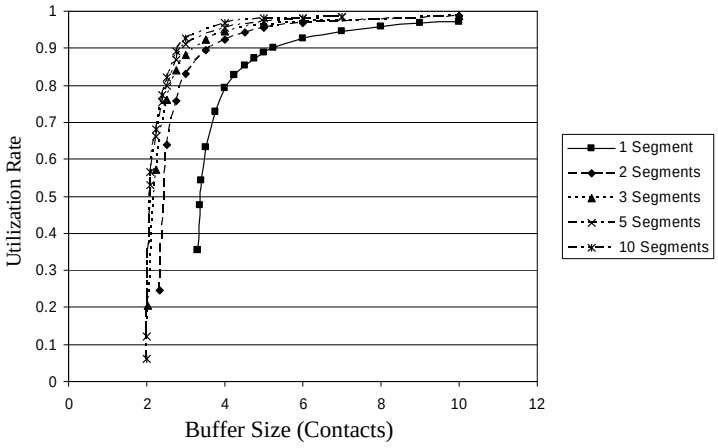

Figure 6. Capacity utilization rate vs. the buffer size for different numbers of segments per pass, 0.25% Data Loss Rate, p=0.895, p_1=0.95.

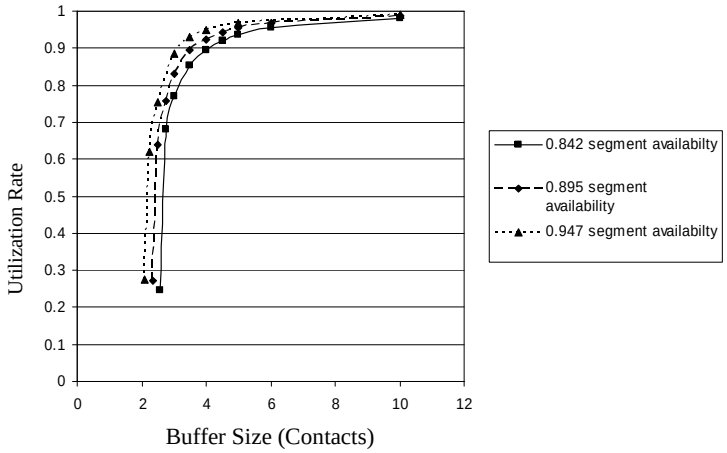

Figure 7. Capacity utilization rate vs. buffer size for different values of segment availability. 2 segments per pass, 0.25% data loss rate, $p1$=0.95

V. Performance Analyis of a System Design: Space Interferometry Mission (SIM) Example

The Space Interferometry Mission (SIM) is scheduled for launch in 2010. Its mission is to find Earth-sized planets orbiting distant stars by observing the movement of those stars for an extended period of time. These obeservations are done using an interferometry suite that generates about 98 Gbits of data per week. As these observations are highly accurate and a complete set of observations over the life of the mission is needed in order to accurately determine the size of the planets, a data loss rate of 0.01% is needed by the mission scientists. The spacecraft will be in an Earth-trailing orbit around the sun and every year its distance from Earth increases by approximately 0.11 au. At the end of its five-year prime mission the spacecraft will be approximately 0.6 au away from Earth. There are also plans for extending the mission for another five years at the end of which the spacecraft will be approximately 1.1 au away from Earth. During the prime mission three passes per week are scheduled on the Deep Space Network's 34-meter Beam Waveguide subnet with each pass tracking the spacecraft for four hours. The minimum tracking elevation for these passes is 20 degrees. During the extended mission it is expected that the number of passes per week and/or their duration will increase in order to accommodate the reduction in the spacecraft data rate due to the increased distance.

As SIM is a high data volume mission and there is not enough spectrum available in the 8.41 GHz X-band, the mission decided to use the 32 GHz Ka-band for its downlink telemetry. The telecom equipment onboard the spacecraft consists of a 35-Watt Ka-band TWTA and a 2-meter parabolic antenna with 55% efficiency. Taking into account circuit losses and the margin carried on the link, the spacecraft has an effective EIRP of 98.4 dBm. Two different solid-state recorders were considered for this mission one with 512 Gbits of capacity another with 300 Gbits of capacity.

Given these end-to-end system parameters, two questions need to be answered:

1. Can either of the buffer sizes accommodate the mission data loss requirement at a) the end of the prime mission b) the end of the extended mission?
2. How should the end-to-end system design change if neither design could satisfy the data completeness requirement for the mission?

To answer these questions first the capacity of a pass needs to be characterized. A deep space link is designed for a fixed value of atmospheric noise temperature. In reality atmospheric noise temeprature is a random variable. The DSN obtains the distribution by collecting zenith noise temperature data with Water Vapor Radiometers (WVR's) and Advanced Water Vapor Radiometers (AWVR) at the three DSN Communication Complexes (DSCCs). These complexes are located at Goldstone in California, Madrid in Spain and Canberra in Australia. Given a distribution of the zenith atmospheric noise temperatures, x-percentile weather refers to the x-percentile value of that distribution. Therefore, a link is designed for a zenith noise temperature value that corresponds to

x-percentile weather is available x-percent of the time. SIM tracking policy is to track the spacecraft with a single downlink rate for elevations above 20 degrees. Therefore, for x-percentile weather, the pass capacity is assumed to be the supportable x-percentile data rate at 20 degrees elevation multiplied by the duration of the pass. As SIM passes are relatively short(four to six hours) in duration, a 1-segment model is used for this analysis with an equipment availability of 95%. Furthermore, since Canberra has the worst weather of all the three sites, its atmospheric noise temperature statistics are used to calculate the pass capacity.

Using this approach first the pass capacities for different weather availabilties were calculated at a distance of 0.6 au based on weather statistics [5] and the antenna performance model in *DSMS Telecommunications Link Design Handbook* [6]. The pass capacity in bits when the pass is available is shown in Figure 8a and the capacity per pass in contacts is shown in Figure 8b for different values of weather availability (p). Note that even though the capacity per available pass is higher for the lower weather availabilities, the average link capacity is lower because of the lower weather availability. This is illustrated in Figure 5. As seen from this figure the maximum average link capacity is achieved at a weather availability of between 70% and 85%. Note that since the increase in distance only changes the scale on the vertical axis of Figure 9, for all distances the maximum average link capacity is achieved at the same weather availabilities.

Given the capacities calculated in Figure 8b, using equations in Section II the data loss rates were calculated for different weather availabilities assuming an equipment availability (p_1) of 95% for buffer sizes of 512 Gbits and 300 Gbits. The results of these calculations are shown in Figures 10 and 11. As seen from Figure 10, both the 300 Gbits and 512 Gbits buffers meet the data loss requirements of the mission at the end of the prime mission. Figure 10 indicates that a link designed for between 95% and 97.5% weather availability has the lowest loss rate. This is due to the fact that the buffer sizes under consideration are quite large (9.18 contacts for the 300-Gbit buffer and 15.67 for 512-Gbit buffer) and the telecom equipment on the spacecraft is powerful enough to provide ample capacity over a 4-hour pass at a distance of 0.6 au. Figure 11 indicates that a link designed to achieve the minimum loss rate requirement for SIM uses on the average less than 70% of the capacity of an available pass. Again, this is due to the large buffer size and ample capacity of the link. Another thing to note is that the highest loss rates are achieved either at very low weather availability values or at very high ones. This results from the following: at low availabilities even though an available pass has a lot of capacity because there are not enough passes to drain the buffer, the buffer overflows causing data losses. Conversely, at very high availabilities the pass is available most of the time but it does not have enough capacity to drain buffer, again causing the buffer to overflow.

The type of analysis presented above has also been applied to the end of the extended mission for SIM. First, analysis was performed to see if the tracking regime during the prime mission (3 4-hour passes per week) meets the data loss rate requirement of for the mission. The results of this analysis are shown in Figures 12a, 12b, 13 and 14. As seen from these figures, the tracking regime during the prime mission does not meet the mission

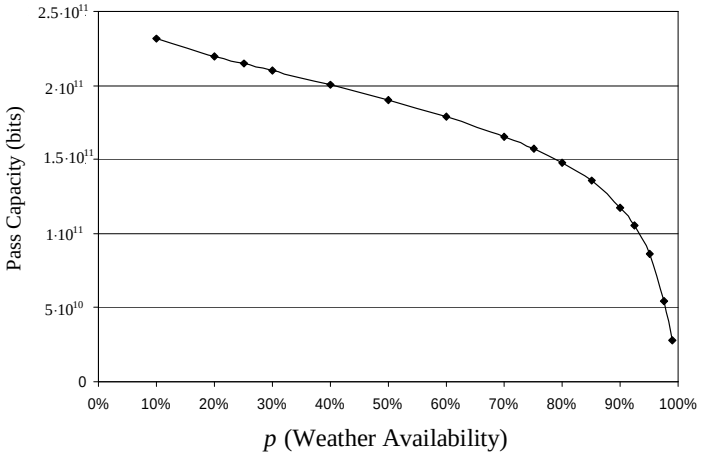

(a) Capacity in bits

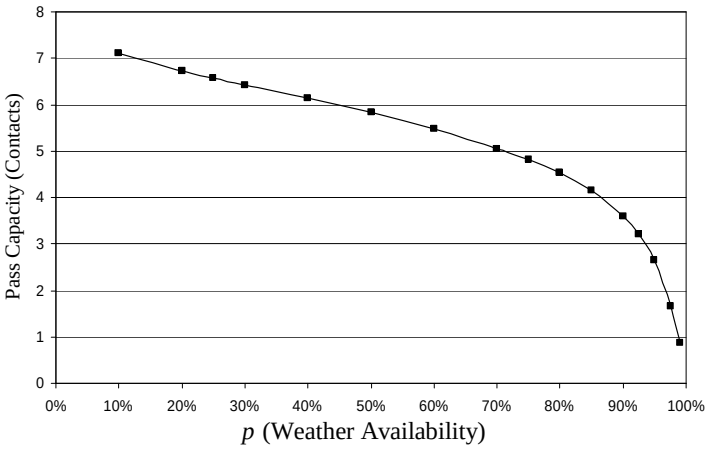

(b) Capacity in contacts, 3 passes per week

Figure 8. Pass capacity vs. p (weather availability) , SIM, 0.6 au distance, Canberra, 4-hour pass duration

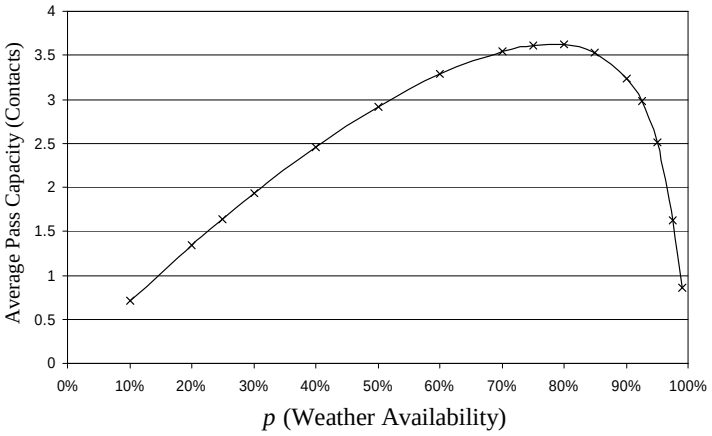

Figure 9. Average pass capacity vs. p (weather availability), SIM, 0.6 au distance, Canberra, 3 passes per week, 4-hour pass duration

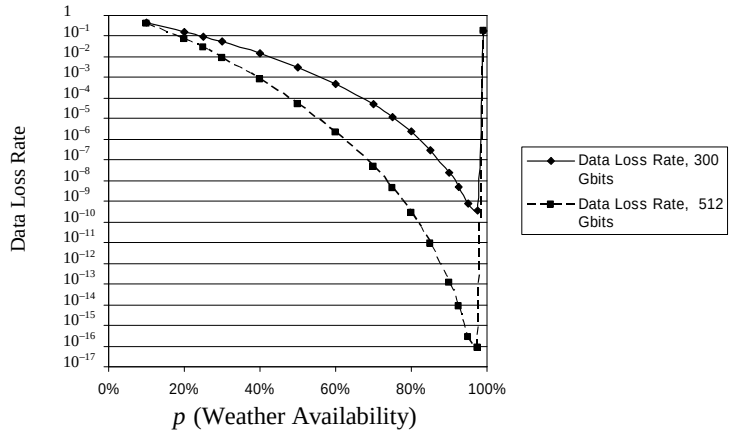

Figure 10. Data loss rate vs. p (weather availability) for different buffer sizes, SIM, 0.6 au distance, 3 4-hour passes per week, 95% equipment availability

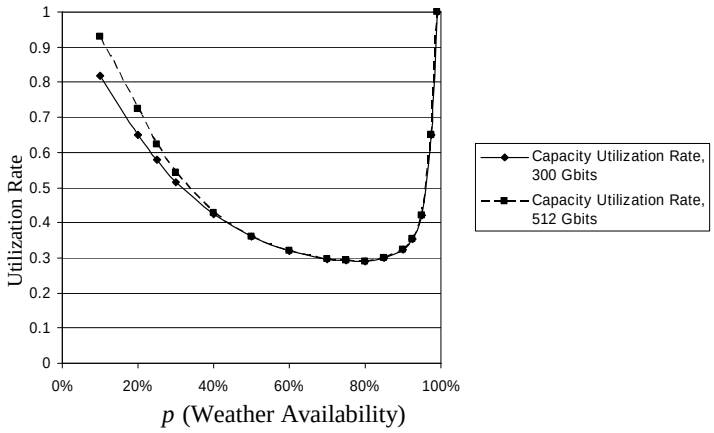

Figure 11. Average capacity utilization rate vs. p (weather availability) for different buffer sizes, SIM, 0.6 au distance, 3 4-hour passes per week, 95% equipment availability

data loss rate requirement with either buffer size at the end of the extended mission. As seen in Figure 12b, this is due to the fact that the capacity per available pass is not sufficiently high. Therefore, the tracking regime must be changed. This change could take the form of either increasing the tracking time per pass or having more frequent passes or a combination of both. Increasing the track time per pass increases only the per pass capacity measured in terms of contacts. Having more frequent passes increases both the buffer size and the per pass capacity in terms of contacts. This occurs because by increasing the number of passes, the amount of data collected between passes decreases thus decreasing the size of a contact. Therefore, even though the capacity of the pass in terms of bits does not change, its capacity in terms of contacts increases. Similarly, even though the size of the buffer in terms of bits does not change, more frequent passes increases its size relative to the number of contacts.

Given this, three tracking regimes were considered for the end of the extended mission:

1. 4 3-hour passes per week.
2. 3 4.5-hour passes per week.
3. 4 3.375-hour passes per week.

For a regime with three passes per week 512-Gbit buffer corresponds to a buffer size of 15.67 contacts and a 300-Gbit buffer corresponds to a buffer size of 9.18 contacts. A regime with four passes per week increases the buffer sizes in terms of contacts to 20.9 contacts for the 512-Gbit buffer and 12.24 contacts for the 300-Gbit buffer.

As usual, first the capacities per available pass for different weather availability values for each regime were calculated. The results of these calculations are shown in Figures 15a and 15b. Note that these figures include the 3 4-hour passes per week tracking regime as a point of comparison. As seen from these figures, although the bit capacity per available pass for the same value of p increases as the pass duration increases, when the frequency of the passes increases, a tracking regime with shorter but more frequent passes could have as

much or more contact capacity per available pass as a tracking regime with longer but less frequent passes. For example, Figure 15b indicates that the tracking regime with 4 3.375-hour passes per week has more contact capacity than the 3 4-hour passes per week regime and as much as 3 4.5-hour passes per week.

Figures 16 and 17 display the data loss rate curves for the different tracking regimes for buffer sizes of 300 Gbits and 512 Gbits, respectively. As these figures indicate with a 300-Gbit buffer only the 4 3.375-hour passes per week tracking regime achieves the data loss rate requirement of 10^{-4} while with a 512-Gbit buffer both the 3 4.5-hour passes per week regime and the 4 3.375-hour passes per week regimes meet the data loss rate requirement. Note that both 4 3.375-hour passes per week regime and 3 4.5-hour passes per week regime have the same number of tracking hours per week. However, because the first tracking regime tracks the spacecraft more frequently, as mentioned above, its buffer size in terms of number of contacts increases thus providing better data loss rate performance. Furthermore, note that while the 4 3-hour passes per week regime has a better performance than the 3 4-hour passes per week regime, neither buffer size achieves the required data loss rate of 10^{-4}.

Looking at Figures 16 and 17 one is tempted to argue that for the same amount of total tracking time it is better to divide the tracking time into short but frequent passes, thus increasing the effective buffer size. While the model does suggest this, this is not feasible both from a theoretical point of view and from a practical aspect. From the theoretical point of view it should be noted that the model used for calculation of the curves in Figures 12 and 13 assume independence of availability of passes. However, as the weather has a large time constant, for more frequent passes this assumption does not hold. From a practical point of view, every time a mission is tracked there is a certain amount pre- and post-pass activities that need to be performed at the tracking station. The duration of these activities is more or less independent of the track duration and its cost is assumed to be fixed per pass. Therefore, a tracking regime with more frequent but shorter passes has a greater cost associated with it than a tracking regime with less frequent but longer passes. However, as less-frequent-but-longer-pass tracking regimes require larger buffer sizes to achieve the same data loss rate as tracking regimes with more frequent but shorter passes, the system designer has to strike a balance between the cost of the spacecraft buffer and the tracking costs.

Of course, looking at figures 10, 13, 16 and 17 two questions arise:

1. Given the spacecraft EIRP and the 3 4-hour passes per week tracking regime and 98 Gbits per week data collection rate, what is the minimum data loss rate for SIM throughout its mission for each of the buffer sizes under consideration?

2. Given the spacecraft EIRP and the 3 4-hour passes per week tracking regime, what is the maximum weekly data collection rate that spacecraft could support throughout its mission for each of the buffer sizes under consideration?

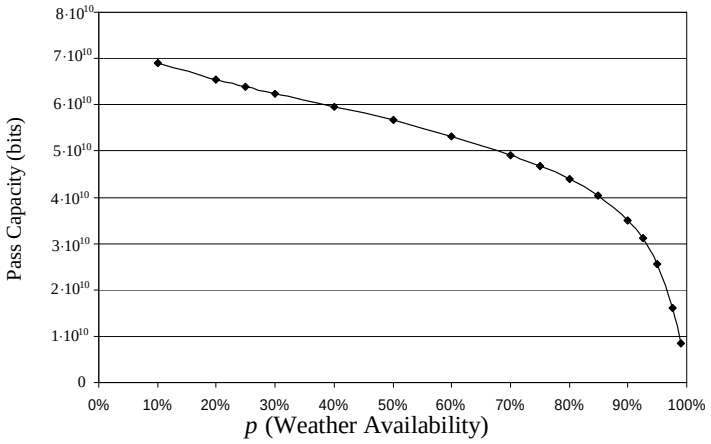

(a) Capacity in bits

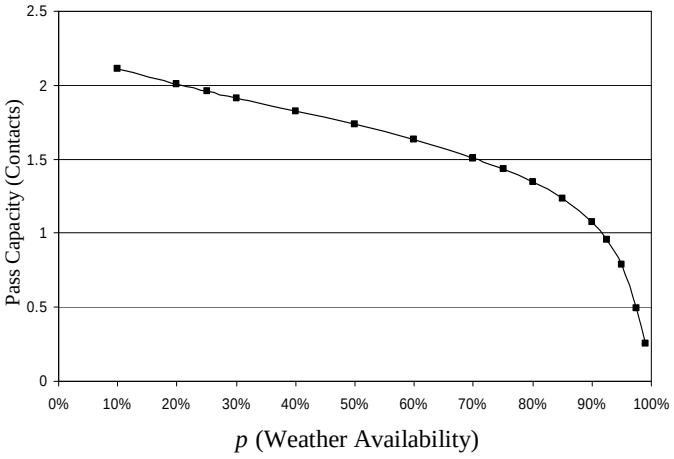

(b) Capacity in contacts, 3 passes per week

Figure 12. Pass capacity vs. p (weather availability) , SIM, 1.1 au distance, Canberra, 4-hour pass duration

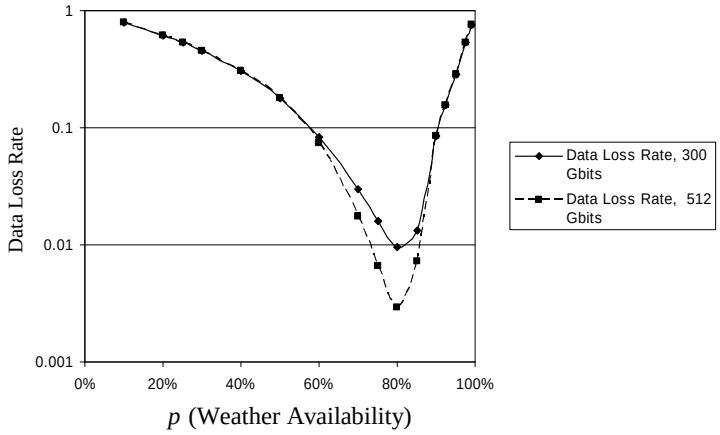

Figure 13. Data loss rate vs. p (weather availability) for different buffer sizes, SIM, 1.1 au distance, 3 4-hour passes per week, 95% equipment availability

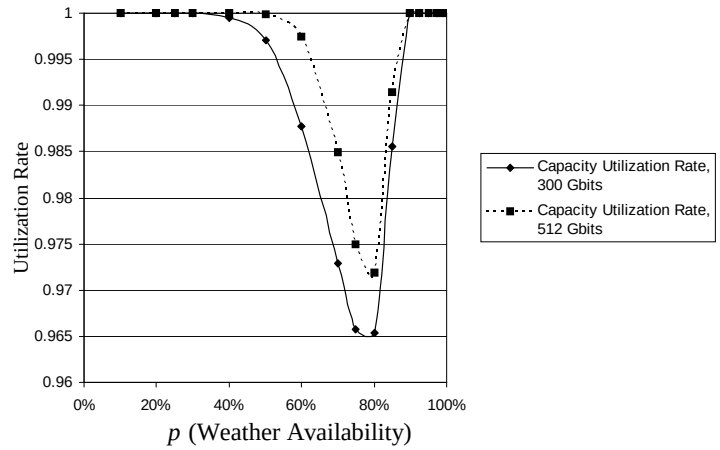

Figure 14. Average capacity utilization rate vs. p (weather availability) for different buffer sizes, SIM, 1.1 au distance, 3 4-hour passes per week, 95% equipment availability

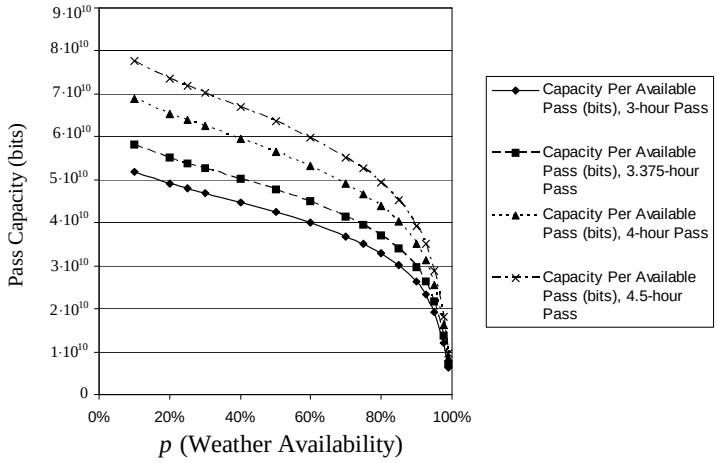

(a) Capacity in bits

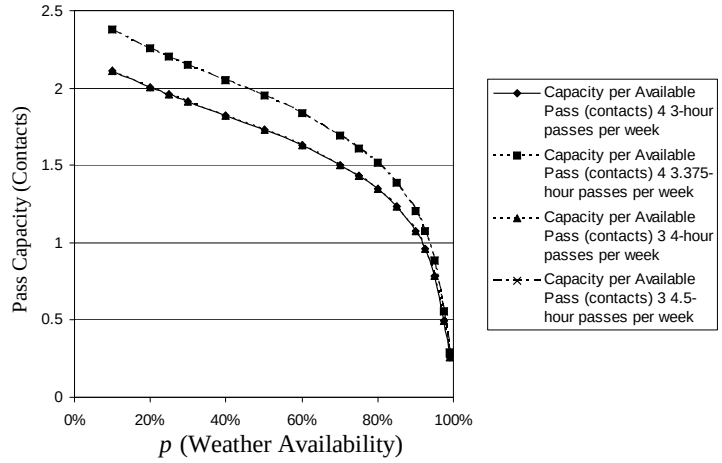

(b) Capacity in contacts

Figure 15. Pass capacity per available pass vs. p (weather availability) for different tracking regimes, SIM, 1.1 au distance

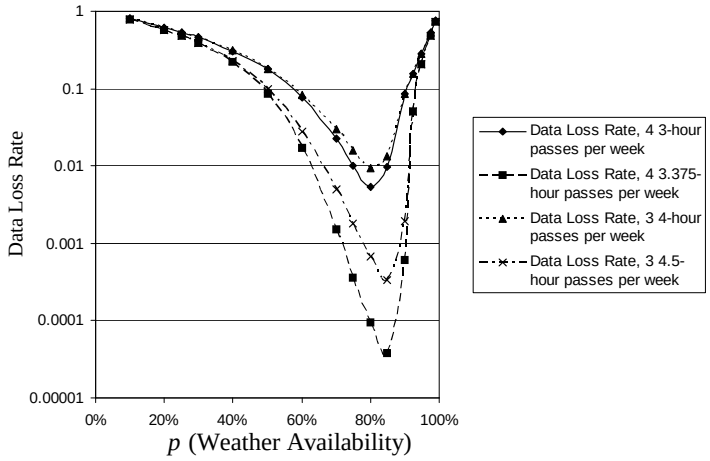

Figure 16. **distance,**

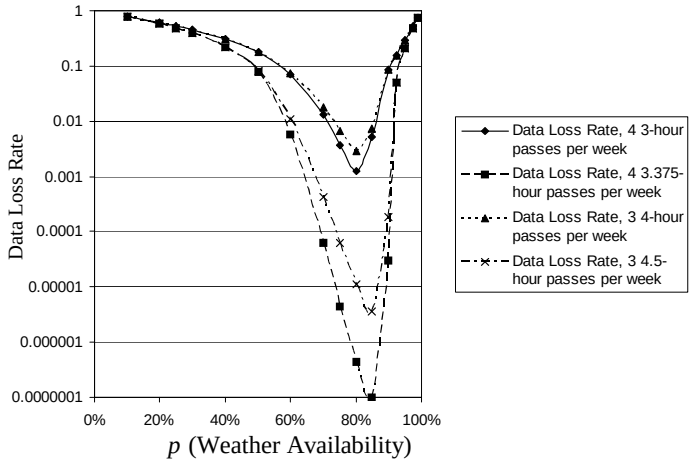

Figure 17. **distance,**

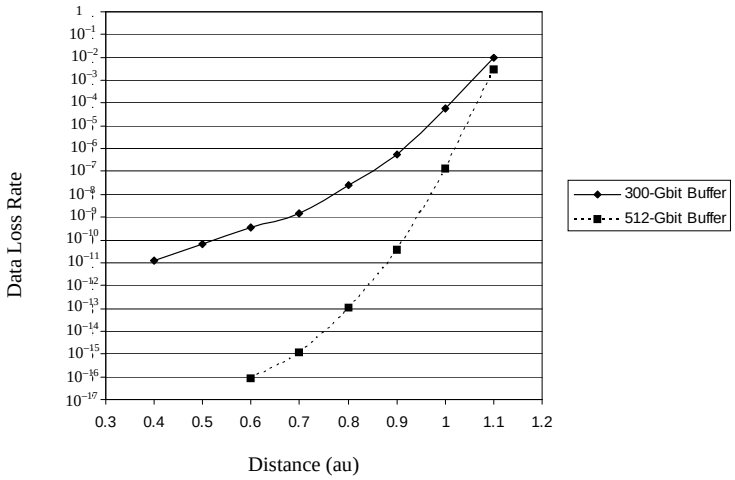

Figure 18. Minimum data loss rate vs. distance for different buffer sizes, SIM, 3 4-hour passes per week, 95% equipment availability, 98 Gbits data collection per week

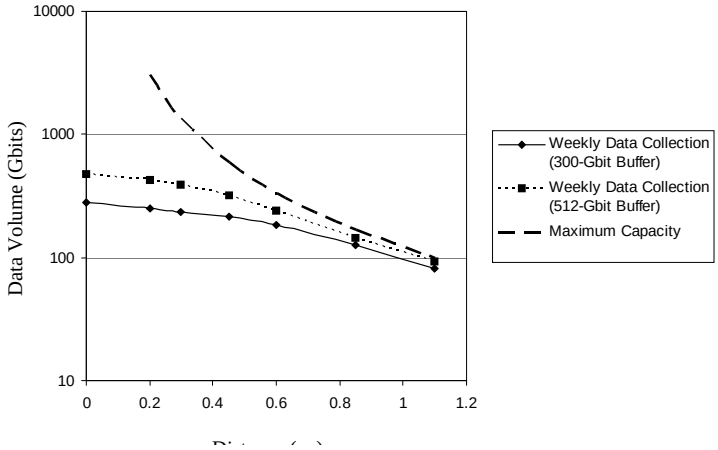

Figure 19 **stance for**

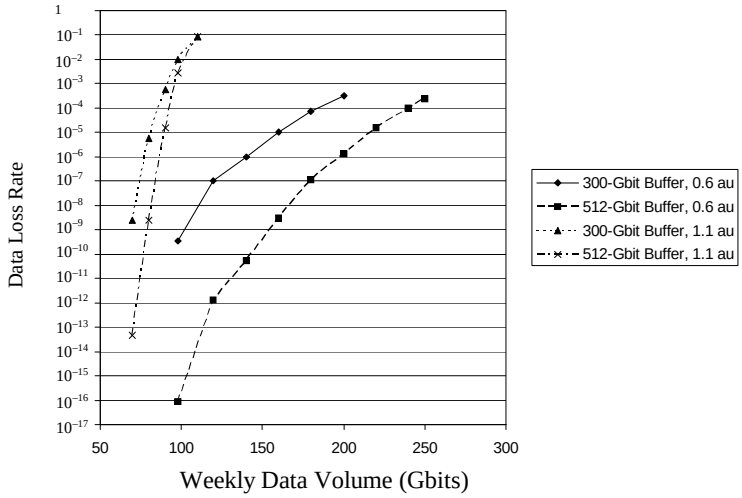

Figure 20. Minimum data loss rate vs. weekly data volume for different buffer sizes at different distances, SIM, 3 4-hour passes per week, 95% equipment availability

The answer to the first question is presented in Figure 18. As seen from this figure as the spacecraft distance from Earth increases so does the data loss rate. With a 300-Gbit buffer the tracking regime meets the minimum data loss requirement of 0.01% at spacecraft-to-Earth distance of slightly less than 1 au. With a 512-Gbit buffer the tracking regime meets the minimum data loss requirement at a distance of slightly greater than 1 au. Furthermore, as the distance increases the difference between the performance of the two buffer sizes becomes less. The explanation for this is as follows: at relatively close distances the received power on the ground is sufficiently high as to reduce probability of weather outage to practically zero and increase capacity to practically infinity. This means that the dominating process causing data losses is equipment failure. Therefore, the data loss rate, P_b, could be calculated from equation 13 with $p_1 = 0.95$, $j_0 = 32.67$ Gbits and $m_{\min}^{(a)}$ equal to either 300 Gbits or 512 Gbits. Using this equation the data loss rate for a 300-Gbit buffer size is 1.62×10^{-12} and for a 512-Gbit buffer it is 1.11×10^{-20}. However, as the spacecraft moves away weather outages and finite link capacity become a significant factors in the data loss process.

The question regarding supportable weekly data volume is answered in figures 19 and 20. Figure 19 displays the maximum supportable weekly data volume for a data loss rate of 0.0001 for 300-Gbit and 512-Gbit buffer sizes as well as maximum average link capacity as a function of distance for SIM. The maximum average weekly link capacity was obtained by obtaining curves similar to Figure 9 at different distances and calculating their maximums and multipying them by 0.95×3 to account for the three weekly passes and 95% equipment availability. As seen from Figure 19, at short distances there is a significant difference between these three curves (especially between the maximum average capacity curve and the supportable data volume curves). However, for longer distances this difference becomes less noticeable. Again, this is due to the fact that at short distances the data loss is primarily caused by equipment failure while at longer distances weather outages and limited link capacity cause much of the data loss. At very short distances since the availability is 100% and the capacity is practically infinite, the maximum supportable data volume could be calaculated by calculating j_0 in equation 13 with $P_b = 0.0001$, $p_1 = 0.95$ and $m_{\min}^{(a)}$ equal to either 300 Gbits or 512 Gbits. The solution to j_0 is obtained easily from Figure 4. As seen in Figure 4, for $P_b = 0.0001$, $m_{\min}^{(a)}$ equals to 3.21 contacts. This means that $j_0 = m_{\min}^{(a)}/3.21$. Since the weekly data volume is $3j_0$ then the weekly supportable data volumes at zero distance are 478.5 Gbits and 280.4 Gbits for buffer sizes of 512 Gbits and 300 Gbits, respectively. Note that as the distance becomes larger, the supportable data volume is reduced, therefore, the relative buffer size approaches infinity. With infinite buffer size, the maximum supportable weekly data volume is equal to the maximum average link capacity divided by $1 - P_b$. Since in this case P_b is small, then at large distances the difference between supportable data volume curves and maximum average weekly capacity becomes negligible.

Figure 20 indicates that at shorter distances the data loss rate is less sensitive to the weekly data collection rate than at longer distances. This is due to the fact that at longer distances the process is dominated by the maximum average weekly link capacity as indicated by Figure 19. To state it in a simplified manner, if the supportable weekly data volume is the same as the average link capacity, all the additional data collected beyond the supportable weekly data volume is not transmitted and therefore lost. Hence, at longer distances the data loss rate is more sensitive to increases in the weekly data volume.

VI. Caveats

While the model presented in this paper provides a useful tool for analyzing the buffer size and the link capacity requirements for a spacecraft, it should be understood that some of the simplifying assumptions made here are not very realistic and the model only provides a first order approximation of these requirements. For example, if the spacecraft does not change its data rate during a pass, the statistical weather availability of that data rate changes with the tracking elevation. In general, the availability is higher for higher elevations than it is for the lower elevations. This means that even though weather may not change appreciably during the pass, because of the increased availablity at higher elevations, bad weather would only cause partial loss of data during the pass.

Furthermore, the assumption about the independence of availability from pass to pass may not be valid. When the equipment breaks down it could be out of service for several days and if no substitute for the equipment is found then a single equipment breakdown may affect several consecutive passes. Similarly, weather can be bad for several days thus affecting several consecutive passes.

Another point to note is that the analysis presented here concerns itself with only one parameter: the data loss rate. However, with most queueing theoretic type of problems data loss rate is usually considered together with the delay. Delay was not considered here because most spacecraft do not have simple data prioritization schemes as the data priority is usually determined dynamically based on prior observations. This means that while a system design may meet the data loss rate requirements based on the models presented here, it may not meet the mission latency requirements. It should be noted that as a rule of thumb, in order to reduce latency, the capacity per available pass and/or pass availablility need to be increased. This means that money has to be spent to provide higher spacecraft EIRP.

Finally, as mentioned in the assumptions, this analysis is mostly applicable for spacecraft with a single type of data. If the spacecraft has multiple data types this analysis needs to be further refined to take into account divergent data loss/latency requirements for each data type.

VII. Conclusions

In this paper equations for a simple Markovian model for the state of the spacecraft buffer have been presented. It was illustrated how this model could be used for the analysis and design of end-to-end spacecraft data systems in terms of their data loss rates. In addition, sensitivity of this model to changes in the spacecraft data collection rate and the spacecraft-to-Earth distance were demonstrated through an example. The results indicate that a larger buffer size adds more versatility to the spacecraft by reducing the senstivity of the telecom system design to changes in the data collection rate, data loss rate requirements and modeling of the channel. Furthermore, it was illustrated that at short distances the data loss process is dominated by the equipment availability and the spacecraft buffer size while at longer distances this process is dominated by the average link capacity.

References

[1] Shambayati, S., "Optimization of a Deep-Space Ka-Band Link Using Atmospheric-Noise-Temperature Statistics," *TMO Progress Report 42-139, July-September 1999*, pp. 1-16, Jet Propulsion Laboratory, Pasadena, CA, November 15, 1999.

[2] Shambayati, S., "Maximization of Data Return at X-Band and Ka-Band on the DSN's 34-Meter Beam-Waveguide Antennas," *IPN Progress Report 42-148, October-December 2001*, pp. 1-20, February 15, 2002.

[3] Shambayati, S., "On the Use of W-Band for Deep-Space Communications," *IPN Progress Report 42-154, April-June 2003*, pp. 1-17, Jet Propulsion Laboratory, Pasadena, CA, August 15, 2003.

[4] Hoel, P. G., Port, S. C. and Stone, C. J., *Introduction to Stochastic Processes*, pp. 84-111, Houghton Mifflin Company, Boston, 1972.

[5] Sniffin, R. W., Ed., *DSMS Telecommunications Link Design Handbook (810-005, Rev. E)*, Module 105, Rev. A: Atmospheric and Environmental Effects, *http://deepspace.jpl.nasa.gov/dsndocs/810-005/105/105A.pdf*, Jet Propulsion Laboratory, Pasadena, CA, December 15, 2002.

[6] Sniffin, R. W., Ed., *DSMS Telecommunications Link Design Handbook (810-005, Rev. E)*, Module 104, Rev. A: 34-m BWG Stations Communications Interfaces, *http://deepspace.jpl.nasa.gov/dsndocs/810-005/104/104A.pdf*, Jet Propulsion Laboratory, Pasadena, CA, February 5, 2004.

[7] Shambayati, S., "Deep-Space Ka-band Link: Design, Continuity and Completeness," *IEEE Aerospace Conference*, Big Sky, Montana, March 1-7, 2008